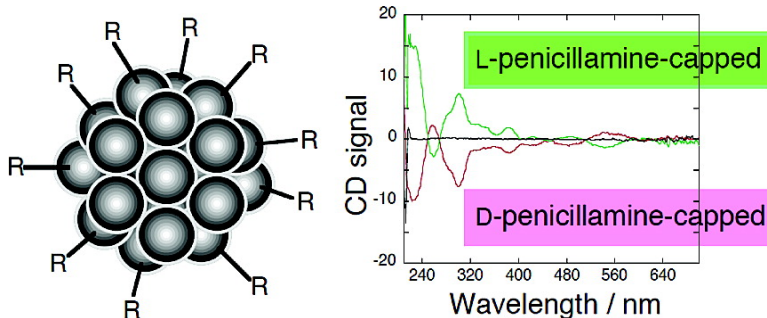


## Large Optical Activity of Gold Nanocluster Enantiomers Induced by a Pair of Optically Active Penicillamines

Hiroshi Yao, Kanae Miki, Naoki Nishida, Akito Sasaki, and Keisaku Kimura

*J. Am. Chem. Soc.*, **2005**, 127 (44), 15536-15543 • DOI: 10.1021/ja053504b • Publication Date (Web): 13 October 2005

Downloaded from <http://pubs.acs.org> on March 25, 2009



### More About This Article

Additional resources and features associated with this article are available within the HTML version:

- Supporting Information
- Links to the 22 articles that cite this article, as of the time of this article download
- Access to high resolution figures
- Links to articles and content related to this article
- Copyright permission to reproduce figures and/or text from this article

[View the Full Text HTML](#)

## Large Optical Activity of Gold Nanocluster Enantiomers Induced by a Pair of Optically Active Penicillamines

Hiroshi Yao,<sup>\*,†</sup> Kanae Miki,<sup>†</sup> Naoki Nishida,<sup>†</sup> Akito Sasaki,<sup>‡</sup> and Keisaku Kimura<sup>†</sup>

Contribution from the Graduate School of Material Science, University of Hyogo, 3-2-1 Koto, Kamigori-cho, Ako-gun, Hyogo 678-1297, Japan, and X-ray Research Laboratory, Rigaku Corporation, 3-9-12 Matsubara-cho, Akishima, Tokyo 169-8666, Japan

Received May 29, 2005; E-mail: yao@sci.u-hyogo.ac.jp

**Abstract:** We have succeeded for the first time in preparing a pair of gold nanocluster enantiomers protected by optically active thiols: D- and L-penicillamine (D-Pen and L-Pen). Circular dichroism (CD) spectroscopy confirmed the mirror image relationship between the D-Pen-capped and the L-Pen-capped gold nanoclusters, suggesting that the surface modifier acts as a chiral selector, and that the nanoclusters have well-defined stereostructures as common chiral molecules do. No CD signals could be obtained when the gold nanoclusters were synthesized by using a racemic mixture (*rac*-Pen). These chiroptical properties were investigated for the three separated fractions of each of the gold nanoclusters (D-Pen-capped, L-Pen-capped, or *rac*-Pen-capped clusters) by polyacrylamide gel electrophoresis (PAGE). Each fractioned component has the mean diameter of 0.57, 1.18, or 1.75 nm that was determined by a solution-phase small-angle X-ray scattering. With a decrease in the mean cluster diameter, optical activity or anisotropy factors gradually increased. On the basis of the kinetic and the structural considerations, the origins of large optical activity of the gold nanocluster enantiomers are discussed.

### 1. Introduction

A material is optically active if it preferentially absorbs or affects the polarization of light passing through it. Specificity in the optical activity is fundamental in chemical biology and pharmacology and has accordingly been widely studied.<sup>1</sup> In organic molecules, optical activity is the result of at least one tetrahedral carbon atom which has four different groups attached to it.<sup>2</sup> Such a carbon is known as a chiral center or an asymmetric carbon. For example, all amino acids, except for glycine, are chiral, and only one form (L-form) is biochemically active. In contrast, inorganic molecules may also contain asymmetric atoms, such as nitrogens, sulfurs, and so forth; however, the chiral center is not absolutely necessary for optical activity in many cases. Overall molecular symmetry (that is, dissymmetric structure) in many metal complex ions leads to optical activity; for example, the mirror image  $\Lambda$  and  $\Delta$  isomers of  $[\text{Co}(\text{en})_3]^{3+}$  (en = ethylenediamine) are well-known.<sup>2</sup>

Nanoclusters are a new class of materials made up of several tens to hundreds of atoms and/or molecules, and thus, they can be seen as intermediate composites between single atoms/molecules and bulk materials. In particular, metal nanoclusters are of considerable interest because some of them show a distinct size dependence in their electronic properties; for example, gold nanoclusters with the diameter reduced to 1–2 nm give discrete

electronic transitions among quantized levels, so that useful nanoelectronic and sensing applications are expected.<sup>3</sup> For geometrical characteristics in such small-sized materials, low-symmetry structures are established to observe chirality for semimetallic carbon fullerenes<sup>4</sup> and nanotubes.<sup>5</sup> In bare and organically modified gold nanoclusters, theoretical calculations predict their structural distortion, resulting in the formation of chiral core nanostructures.<sup>6</sup> These studies also show that gold cores in the methylthiolate-capped clusters exhibit more chirality than the corresponding bare clusters. Whetten and co-workers experimentally observed intense optical activity in gold nanoclusters protected by a monolayer of glutathione molecules.<sup>7</sup> The gold nanoclusters with the core diameter smaller than ~2 nm (~10–40 kDa in mass, where 1 kDa corresponds to the mass of approximately five Au atoms) were prepared and isolated as a discrete family of mass-selected fractions. These nanoclusters were small enough to have discrete electronic states not found in larger particles and displayed circular dichroism

<sup>†</sup> University of Hyogo.

<sup>‡</sup> Rigaku Corporation.

(1) Sheldon, R. A. *Chirotechnology*; Dekker: New York, 1993.

(2) (a) Lambert, J. B.; Shurvell, H. F.; Verbit, L.; Cooks, R. G.; Stout, G. H., *Organic Structural Analysis*; Macmillan: New York, 1976. (b) Shriver, D. F.; Atkins, P. W.; Langford, C. H. *Inorganic Chemistry*, 2nd ed.; Oxford University Press: Oxford, 1994.

(3) (a) Chen, S.; Ingram, R. S.; Hostetler, M. J.; Pietron, J. J.; Murray, R. W.; Schaaff, T. G.; Khoury, J. T.; Alvarez, M. M.; Whetten, R. L. *Science* **1998**, *280*, 2098. (b) Schwerdtfeger, P. *Angew. Chem., Int. Ed.* **2003**, *42*, 1892. (c) Whetten, R. L.; Shafiqullin, M. N.; Khoury, J. T.; Schaaff, T. G.; Vezmar, I.; Alvarez, M. M.; Wilkinson, A. *Acc. Chem. Res.* **1999**, *32*, 397. (d) Huang, T.; Murray, R. W. *J. Phys. Chem. B* **2001**, *105*, 12498.

(4) Ettl, R.; Chao, I.; Diederich, F.; Whetten, R. L. *Nature* **1991**, *353*, 149.

(5) Iijima, S. *Nature* **1991**, *354*, 56.

(6) (a) Garzón, I. L.; Reyes-Nava, J. A.; Rodríguez-Hernández, J. I.; Sigal, I.; Beltrán, M. R.; Michaelian, K. *Phys. Rev. B* **2002**, *66*, 073403. (b) Garzón, I. L.; Beltrán, M. R.; González, G.; Gutiérrez-González, I.; Michaelian, K.; Reyes-Nava, J. A.; Rodríguez-Hernández, J. I. *Eur. Phys. J. D* **2003**, *24*, 105. (c) Román-Velázquez, C. E.; Noguez, C.; Garzón, I. L. *J. Phys. Chem. B* **2003**, *107*, 12035.

(7) (a) Schaaff, T. G.; Knight, G.; Shafiqullin, M. N.; Borkman, R. F.; Whetten, R. L. *J. Phys. Chem. B* **1998**, *102*, 10643. (b) Schaaff, T. G.; Whetten, R. L. *J. Phys. Chem. B* **2000**, *104*, 2630.

(CD) from the ultraviolet to the infrared. Note that glutathione is an optically active tripeptide of L-L configuration ( $\gamma$ -L-glutamyl-L-cysteinyl-glycine). Since they have prepared gold nanoclusters protected by only one of the enantiomeric species, the origins of optical chirality or chiroptical properties are not well understood yet and are still an object of scientific activity. Hence, the gold nanoclusters protected by a pair of well-defined enantiomers (that is, both L- and D-form optical isomers) are required.

In this article, we report the synthesis of hydrophilic, optically active gold nanoclusters protected by an enantiopure D- or L-form thiol as well as a racemic (DL) thiol. We found that chiroptical properties of the gold nanoclusters are strongly dependent on the stereochemistry of the surface modifier and show the clear *mirror image* relationship between the homochiral gold nanoclusters, proving that the surface modifier acts as a chiral selector for small gold nanoclusters. Origins of the optical activity will be discussed from a viewpoint of a chiral core model or a dissymmetric vicinal effect.

## 2. Experimental Section

**Chemicals.** Hydrogen tetrachloroaurate tetrahydrate ( $\text{HAuCl}_4 \cdot 4\text{H}_2\text{O}$ , 99%), sodium borohydride ( $\text{NaBH}_4$ , >90%), methanol (GR grade), and ethanol (GR grade) were received from Wako Pure Chemicals and used as received. Electrophoresis grade acrylamide,  $N,N'$ -methylenebisacrylamide (Bis), tris(hydroxymethylaminomethane) (Tris), glycine, ammonium peroxydisulfate (APS), and  $N,N,N',N'$ -tetramethylethylenediamine (TEMED) were received from Nacalai Tesque and used without further purification. Enantiopure D- or L-penicillamine ( $\text{Me}_2\text{-C}(\text{SH})\text{-CH}(\text{NH}_2)\text{COOH}$ ; abbreviated as D-Pen (99%) or L-Pen (99%), respectively) and racemic DL-penicillamine (abbreviated as *rac*-Pen (97%)) were received from Aldrich and used as received. The chemical structures of D- and L-Pen are shown in Figure 1a. In the formulas, “\*” denotes an asymmetric carbon. Pure water was obtained by an Advantec GS-200 automatic water-distillation supplier.

**Synthesis of Penicillamine-Capped Gold Nanoclusters.** Each of three kinds of penicillamines (D-form, L-form, and racemate) was used as a surface modifier. Briefly, 0.5 mmol of  $\text{HAuCl}_4$  dissolved in water (0.121 M) and 1.0 mmol of penicillamine (D-, L-, or *rac*-Pen) were at first mixed in methanol (100 mL), followed by the addition of a freshly prepared 0.2 M aqueous  $\text{NaBH}_4$  solution (25 mL) under vigorous stirring.<sup>8</sup> After further stirring for 1.5 h, the solution was stored overnight. Addition of ethanol (300 mL) into the stored solution gave a dark-brown crude precipitate. The precipitate was then thoroughly washed with water/ethanol (1/9) and ethanol. Finally, a nanocluster powder was obtained by a freeze-drying procedure. The gold nanocluster sample prepared by using D-Pen, L-Pen, or *rac*-Pen is termed as Au-D-Pen, Au-L-Pen, or Au-*rac*-Pen, respectively.

**Electrophoresis.** Electrophoresis is a useful technique applicable to separate or purify large-sized molecules or clusters that differ in size, charge, or conformation.<sup>7a,9</sup> We applied polyacrylamide gel electrophoresis (PAGE) using a slab gel unit which employs a gel of 2 mm thickness (ATTO, AE-6200). For the stacking and the separating gels, the total contents of the acrylamide monomers were 3% (acryl-

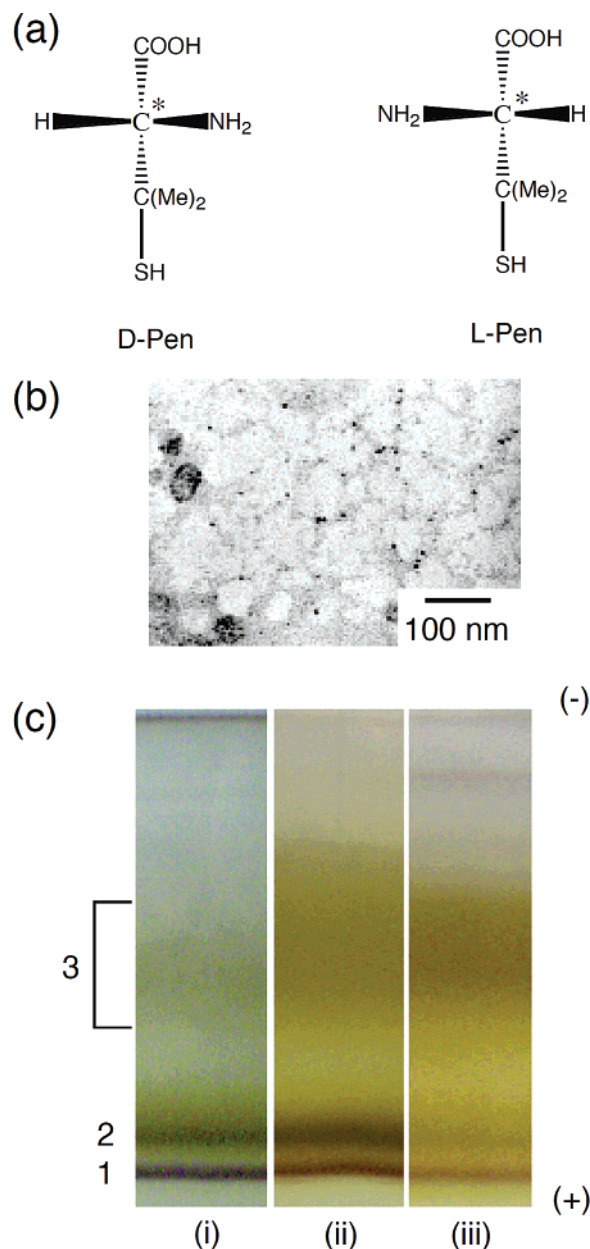


**Figure 1.** (a) Chemical structure of D- or L-penicillamine (D-Pen or L-Pen). (b) TEM image of the as-prepared Au-D-Pen. (c) Photographs of the PAGE separation. Three bands are labeled in the order of mobility of nanoclusters (1 being most mobile). (i), (ii), and (iii) show the results for Au-D-Pen, Au-L-Pen, and Au-*rac*-Pen samples, respectively.

amide/Bis = 93/7) and 28% (acrylamide/Bis = 93/7), respectively. The stacking and the separating gels were buffered at pH = 6.8 and 8.7 with Tris-HCl solution, respectively. The running electrode buffer consisted of glycine (192 mM) and Tris (25 mM) solution. The as-prepared product of penicillamine-capped gold nanoclusters was dissolved in a buffer solution (pH = 6.8) at a concentration of 4 mg/mL. The sample solution was loaded onto a stacking gel top and eluted for ~6 h at a constant voltage mode (150 V) controlled using a power supply (ATTO, AE-8150) to achieve separation. To extract gold nanoclusters in aqueous solution, a part of the gel containing each fraction was cut out and homogenized, followed by the addition of distilled water and stayed overnight. The gel lumps were removed by centrifugation.

**Instrumentation.** Transmission electron microscopy (TEM) was conducted with a Hitachi-8100 electron microscope operating at 200 kV. FT-IR spectra were measured with a Horiba FT-720 infrared

(8) We have revealed that the size control of gold nanoparticles in the range of 1–4 nm was accomplished by varying the molar ratio of the surface modifier (mercaptosuccinic acid, MSA) to gold (S/Au) during the nanoparticle formation process (Chen, S.; Kimura, K. *Langmuir* **1999**, *15*, 1075.). On the basis of the study, we prepared Pen-capped gold nanoclusters at a different S/Au ratio (=1) from that described in the Experimental Section (S/Au = 2). According to the result on spectroscopic measurements, the Pen-capped gold nanoclusters prepared at S/Au = 1 showed a smooth and structureless absorption spectrum, indicating a broader size distribution compared to the samples prepared at S/Au = 2. Hence, we focused on the nanocluster samples described in the text.

(9) Negishi, Y.; Takasugi, Y.; Sato, S.; Yao, H.; Kimura, K.; Tsukuda, T. *J. Am. Chem. Soc.* **2004**, *126*, 6518.



spectrophotometer. For the measurements, a KBr disk pellet containing the as-prepared gold nanocluster powder was prepared. Absorption spectra were recorded with a Hitachi U-4100 spectrophotometer. CD spectra were recorded with a JASCO J-720 spectropolarimeter using a bandwidth of 2 nm. The ellipticity resolution is 0.01 mdeg. In the CD measurement, absorption spectrum was simultaneously recorded. Rectangular 1 cm cuvettes made of quartz were used for the measurements.

#### Determination of the Size Distribution of Gold Nanoclusters.

Particle size distributions of gold nanoclusters were determined by the small-angle X-ray scattering (SAXS) technique in solution, where the details were described elsewhere.<sup>10a,c</sup> Briefly, the SAXS profile of gold nanoclusters dispersed in solution was first measured, followed by analyzing the profile based on the assumption that the size distribution is approximated by the  $\Gamma$  distribution function.

When the scatter is a sphere with a diameter of  $D$ , the scattering intensity,  $I(q, D_0, M)$ , is expressed by eq 1<sup>10a</sup>

$$I(q, D_0, M) = (\Delta\rho)^2 \int_0^\infty \left| \frac{4\pi}{3} \left[ \sin\left(\frac{qD}{2}\right) - \frac{qD}{2} \cos\left(\frac{qD}{2}\right) \right] \right|^2 P(D) dD \quad (1)$$

where  $\Delta\rho$  and  $q$  are the difference between the electron densities of the scatter and the solution matrix and the scattering vector, respectively. For the solution-phase gold nanoclusters protected by organic ligands, the X-ray scattering is dominated by the metal core with a large electron density, so that we can determine the core size of the gold nanoclusters by this method.<sup>10a,b</sup> The  $\Gamma$  distribution function,  $P(D)$  in eq 1, is expressed as follows

$$P(D) = \frac{1}{\Gamma(M) \left(\frac{D_0}{M}\right)^M} \exp\left(-\frac{D}{D_0} M\right) D^{M-1} \quad (2)$$

$$\Gamma(M) = \int_0^\infty x^{M-1} e^{-x} dx \quad (3)$$

where  $M$  is the shape parameter that relates to the dispersion of the estimated diameters.  $\Gamma(M)$  is the gamma function, and  $D_0$  denotes the mean diameter of the scatter (that is, the gold core). Hence,  $D_0$  and  $M$  are determined based on the SAXS profile simulation using eqs 1–3.

### 3. Results and Discussion

**Chemical Characterization.** As-prepared sample analyses clarify the chemical and surface properties of penicillamine-capped gold nanoclusters. On the basis of the IR absorption measurements for pure penicillamines and penicillamine-capped gold nanoclusters, we have revealed the following results on the surface chemistry of nanoclusters: penicillamine (D-, L-, or *rac*-Pen) molecules anchor on the gold nanocluster surface through the sulfur atom in the SH group (as revealed by the disappearance of the S–H stretch mode at  $\sim 2570$   $\text{cm}^{-1}$ ). The surface-capping agents on nanocluster surfaces contain carboxylate ( $\text{COO}^-$ ) and primary amino ( $\text{NH}_2$ ) groups, which was confirmed by the presence of characteristic peaks for the stretch modes of  $\text{COO}^-$  ( $\sim 1390$  and  $\sim 1590$   $\text{cm}^{-1}$ ) and those for the N–H stretch ( $\sim 3420$   $\text{cm}^{-1}$ ) and the N–H bending ( $\sim 1630$   $\text{cm}^{-1}$ ) of  $\text{NH}_2$  (see Supporting Information for more details).<sup>11</sup>

Figure 1b shows a typical TEM image of the as-prepared Au-D-Pen sample. The particles with very small diameters ( $\sim 1$ – $2$  nm) are discernible in the image. Note that similar TEM images could be obtained for the as-prepared Au-L-Pen and Au-*rac*-Pen samples. These results show direct evidence for nanocluster formation. However, we could not determine the cluster size distributions for these samples via TEM measurements because particle sizes were too small to exactly analyze.

**Electrophoresis.** Photographs of a typical PAGE separation for Au-D-Pen, Au-L-Pen, and Au-*rac*-Pen samples are shown in Figure 1c.<sup>12</sup> Three bands (reddish, greenish, and brownish bands; the brownish bands are distributed diffusively in the gel) were readily observable under normal illumination for each sample and were located at the same position with each other, suggesting that the prepared gold nanoclusters are composed of similar size components.<sup>7,9</sup> Note that a pale yellow band was likely to appear in front of the reddish component; however, the amount of this band fraction was too small to identify, so that we focus on those three bands. On the basis of the electrophoretic mobility of the nanocluster compounds, the separated compounds are referred to as compounds **1**–**3**, with **1** being the most mobile reddish species. In the case of distinguishing these compounds in regard to the stereochemistry of the surface modifiers, a suffix D, L, or *rac* is added at the end of the compound number; for example, **1<sub>D</sub>**, **2<sub>D</sub>**, and **3<sub>D</sub>** for the Au-D-Pen nanocluster sample.

Size distributions of the fractioned nanoclusters were determined by a solution SAXS measurement. Because all samples exhibited identical band positions (**1**–**3**) in the separating gel, we representatively conducted the size analysis for the compounds **1<sub>D</sub>**, **2<sub>D</sub>**, and **3<sub>D</sub>**. Figure 2a shows the experimental scattering profiles of the components **1<sub>D</sub>**, **2<sub>D</sub>**, and **3<sub>D</sub>** along with the simulated curves. The simulated curves well reproduced the scattering profiles using the  $\Gamma$  distribution function. The obtained parameters are as follows: **1<sub>D</sub>** for  $D_0 = 0.57$  nm ( $M = 6.25$ ), **2<sub>D</sub>** for  $D_0 = 1.18$  nm ( $M = 68.3$ ), and **3<sub>D</sub>** for  $D_0 = 1.75$  nm ( $M = 23.0$ ). The obtained size distributions are shown in Figure 2b. As expected, the compound **1** is the smallest. Hence, these analyses indicate that the compounds were separated by differing core size (with the smallest having the highest mobility). By assuming the density of bulk gold (60 atoms/ $\text{nm}^3$ ),<sup>13</sup> the average number of atoms of the compounds **1**, **2**, and **3** are estimated to be  $\sim 6$ ,  $\sim 50$ , and  $\sim 150$  atoms, respectively. Interestingly, the obtained total numbers of Au atoms in compounds **2** and **3** are very close to the full shell clusters: two shells for 55 atoms, and three shells for 147 atoms.<sup>13</sup> Note that compound **1** (the smallest one) seems to have a broad size distribution compared to that of compound **2**; however, this would be an apparent observation caused by a deviation from the spherical shape assumption of nanoclusters in the simulation.<sup>10</sup> Compounds **1** and **2** clearly showed a single sharp band in the PAGE separation, so that their size distributions should be intrinsically narrow.<sup>7,9</sup>

**Absorption Spectroscopy.** Graphs a–c of Figure 3 show the absorption spectra for the separated compounds (**1**–**3**) of

- (10) (a) Nagao, O.; Harada, G.; Sugawara, T.; Sasaki, A.; Ito, Y. *Jpn. J. Appl. Phys.* **2004**, *43*, 7742. (b) Hostetler, M. J.; Wingate, J. E.; Zhong, C.-J.; Harris, J. E.; Vachet, R. W.; Clark, M. R.; Londono, J. D.; Green, S. J.; Stokes, J. J.; Wignall, G. D.; Glish, G. L.; Porter, M. D.; Evans, N. D.; Murray, R. W. *Langmuir* **1998**, *14*, 17. (c) SAXS measurements were conducted with a Rigaku ATX diffractometer with Cu K $\alpha$  irradiation using a rotating anode X-ray generator.
- (11) (a) Yao, H.; Kojima, H.; Sato, S.; Kimura, K. *Langmuir* **2004**, *20*, 10317. (b) Silverstein, R. M.; Bassler, G. C.; Morrill, T. C. *Spectrometric Identification of Organic Compounds*, 6th ed.; John Wiley & Sons: New York, 1997.

- (12) During the PAGE separation, a small amount of nanocluster agglomerates often remained at the interface of the stacking and the separating gels; however, the yield of the final products (compounds **1** + **2** + **3**) would be  $> \sim 90\%$  as judged from the absorption color.
- (13) Gutierrez, E.; Powell, R. D.; Furuya, F. R.; Hainfeld, J. F.; Schaaf, T. G.; Shafiqullin, M. N.; Stephens, P. W.; Whetten, R. L. *Eur. Phys. J.* **1999**, *D9*, 647.

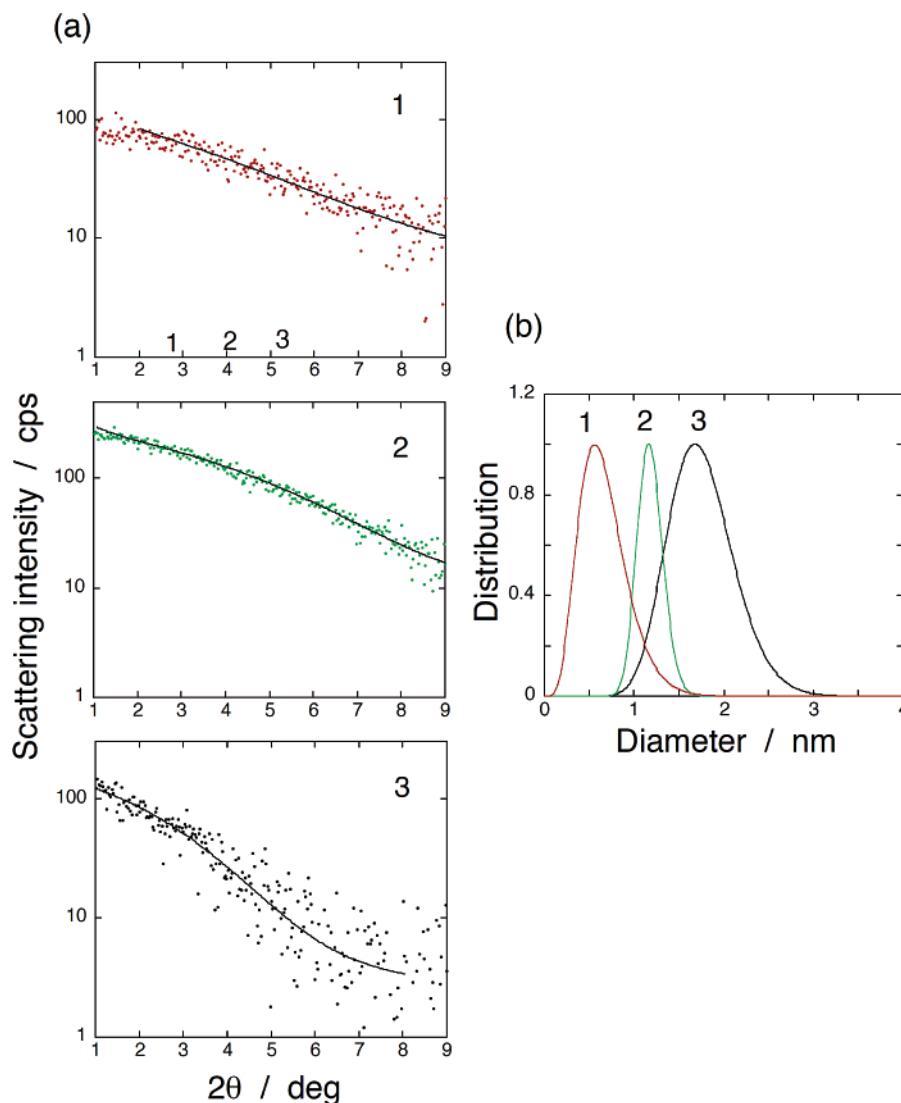


**Figure 2.** (a) X-ray scattering intensity profiles of each numbered gold nanocluster compound. The experimental and the simulated profiles are shown by dots and curves, respectively. (b) Obtained cluster size distributions of each numbered compound.

Au-D-Pen, Au-L-Pen, and Au-*rac*-Pen, respectively, in aqueous solution. The spectral shapes of the separated compounds are almost identical within the same compound numbers, supporting again the fact that each numbered compound has similar particle size. To examine the spectral similarity among the separated nanoclusters in more detail, first derivative spectroscopy was carried out.<sup>14</sup> The insets in Figure 3 show the first derivative absorption spectra of the respective compounds. Identical patterns of the first derivative spectra within the same compound numbers confirm the similarity in their optical response. In stark contrast with gold nanoparticles whose diameters are larger than  $\sim 2$  nm that exhibit a single surface plasmon band at around 520 nm,<sup>15</sup> the spectra (ordinary and the first derivative) for compounds **1** (**1<sub>b</sub>**, **1<sub>L</sub>**, or **1<sub>rac</sub>**) and **2** (**2<sub>b</sub>**, **2<sub>L</sub>**, or **2<sub>rac</sub>**) are structured, whereas compound **3** (**3<sub>b</sub>**, **3<sub>L</sub>**, or **3<sub>rac</sub>**) is less pronounced. In addition, clear absorption onsets appeared in the near-IR region for the compounds **1** and **2**:  $\sim 800$  nm for **1** and  $\sim 840$  nm for

**2**. The onsets are followed by distinct humps, which tend to be blue shifted with a decrease in the core size ( $\sim 580$  nm for **1** and  $\sim 685$  nm for **2**). The results indicate that electronic structures of compounds **1** and **2** are quantized (that is, the observed peaks are substantially ascribed to electronic transitions between the quantized electronic states) and are better viewed as nonmetallic clusters rather than metallic particles protected by thiols. Actually, it is reported that metal to nonmetal transition occurs in the 28–55 gold atom range,<sup>16</sup> consistent with our observations.

To fully understand the exact origin of electronic transitions, we have to determine the total structure and subsequent quantum calculations.<sup>6</sup> However, recent theoretical and experimental studies of monolayer-capped gold nanoclusters allow us to speculate the characteristic features in the optical spectrum.<sup>17</sup> For example, density functional calculations predicted that methylthiolate-covered Au<sub>13</sub> nanoclusters show two distinct peaks at 532 and 395 nm in the visible region. These peaks are

(14) The derivative spectroscopy can reveal spectral details (including peak or shoulder positions) that are not clarified in an ordinary absorption spectrum.

(15) Hostetler, M. J.; Wingate, J. E.; Zhong, C.-J.; Harris, J. E.; Vachet, R. W.; Clark, M. R.; Londono, J. D.; Green, S. J.; Stokes, J. J.; Wignall, G. D.; Glush, G. L.; Porter, M. D.; Evans, N. D.; Murray, R. W. *Langmuir* **1998**, *14*, 17.

(16) (a) Smith, B. A.; Zhang, J. Z.; Giebel, U.; Schmid, G. *Chem. Phys. Lett.* **1997**, *270*, 139. (b) Link, S.; El-Sayed, M. A.; Schaaff, T. G.; Whetten, R. L. *Chem. Phys. Lett.* **2002**, *356*, 240.

(17) Nobusada, K. *J. Phys. Chem. B* **2004**, *108*, 11904.

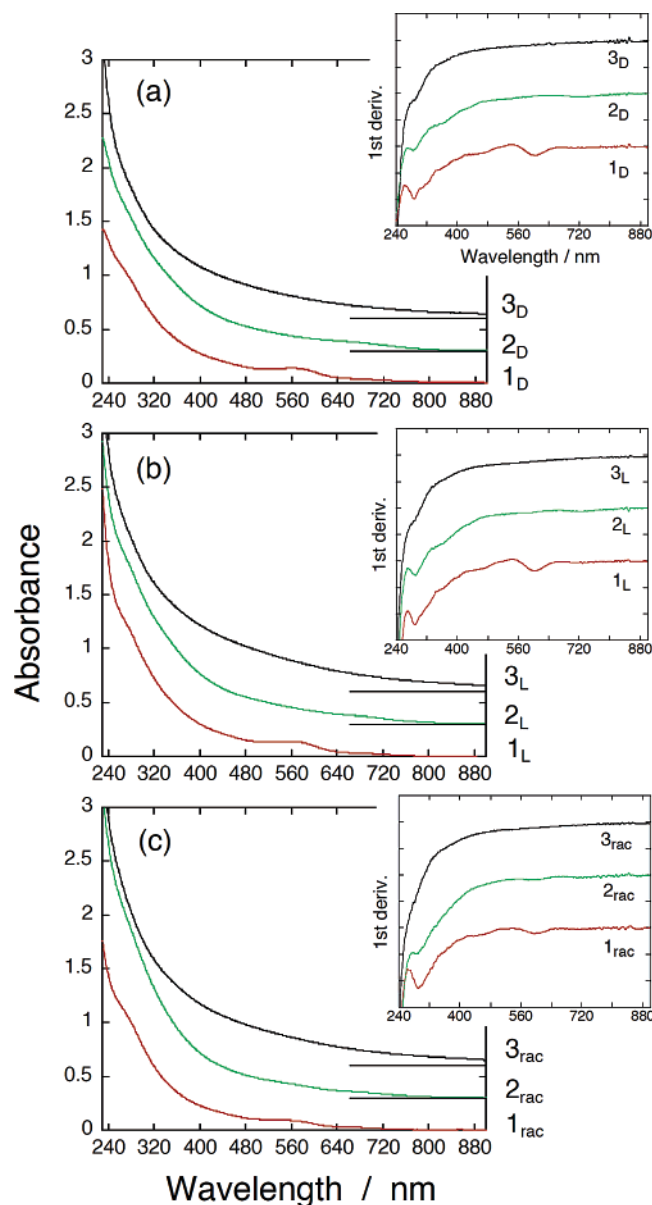


**Figure 3.** Graphs (a), (b), and (c) show the absorption spectra of separated gold nanoclusters for the Au-D-Pen, Au-L-Pen, and Au-*rac*-Pen samples, respectively. For clarity, the spectra for 2 and 3 were off-set by adding a constant. The insets show the first derivative spectra of the respective nanocluster compounds.

assigned to the transitions from the high-lying occupied Au 6s orbitals (HOMO) to the low-lying unoccupied Au 6sp orbitals (LUMO). According to the theoretical study, Tsukuda and co-workers assigned the distinct peaks observed at 730–330 nm for glutathione-protected Au<sub>n</sub> (*n* = 10–39) nanoclusters to be due to the 6s–6sp transitions.<sup>18</sup> Considering this criterion, we can also assign the prominent peak at 580 (compound 1) or 685 nm (compound 2) to be due to the Au 6s–6sp (HOMO–LUMO) transitions between discrete levels.

Recently, it has been elucidated that optical properties of gold nanoclusters are strongly dependent on not only their chemical compositions<sup>18</sup> but also their geometries (or shapes).<sup>19,20</sup> In our samples, each numbered fraction of D-Pen-capped, L-Pen-

capped, and *rac*-Pen-capped gold nanoclusters was located at the identical positions in the separating gel with each other, so that it would have the same chemical compositions within the same compound number.<sup>7,9,18</sup> Therefore, the observed similarity in the absorption spectra suggests that the geometries of gold nanoclusters having the same compound number are almost identical with each other.

**Enantiopure Gold Nanoclusters: CD Spectroscopy.** To obtain significant information on optical activity of the gold nanoclusters, CD spectra of each numbered gold compound were measured in solution over the 210 to 700 nm region (Figure 4a).<sup>21</sup> Reasonably, all compounds of gold nanoclusters protected by a racemate (**1<sub>rac</sub>**–**3<sub>rac</sub>**) did not exhibit CD signals. An equimolar mixture of two homochiral nanoclusters (that is, a mixture of pure D-Pen-capped and L-Pen-capped gold nanoclusters) can cancel out the net optical activity; however, it is implausible because statistical adsorption of thiol molecules onto gold surfaces (that is, the adsorption probability of D-form thiols onto gold surfaces is equal to that of L-form isomers) is proved to be general.<sup>22</sup> Hence, the surface modifier *rac*-Pen would cover the gold nanocluster surface statistically, resulting in the disappearance of circular dichroism. On the other hand, all separated compounds for Au-D-Pen and Au-L-Pen showed considerably complicated CD behaviors. For example, the spectrum of compound **1<sub>b</sub>** shows six minima and six maxima. It would be hard to assign the origins of optical activity in the gold nanoclusters without their structural information. However, the structured CD spectra observed in the visible region should be caused through the different quantized transitions and their interactions in the gold clusters since the optically active surface modifier (D-Pen or L-Pen) contributes to the CD signal only in the UV region (the ordinary absorption and CD spectra of penicillamine enantiomers are shown in Figure 4b). It should be emphasized that the CD signal of compound **1<sub>L</sub>** shows an almost complete mirror image of the ellipticity of **1<sub>b</sub>**. The mirror image relationship in CD signals means that enantiomeric surface modifiers can produce the corresponding enantiomeric gold nanoclusters. This finding indicates that the separated nanoclusters have well-defined stereostructures as common molecules do. Hence, we conclude that the structures of penicillamine-capped gold nanoclusters are stereochemically controlled.

A CD spectrum exhibits the difference of two absorption spectra ( $\Delta A$ ): one measured with left-circularly polarized light and the other one with right-circularly polarized light, and expressed as  $\Delta A = \Delta\epsilon \times c \times l$ , where  $\Delta\epsilon$ , *c*, and *l* denote the molar dichroic absorption, the solute concentration, and the optical path length, respectively. Because the ellipticity  $\theta$  (in degrees) can be expressed as  $33 \times \Delta A$ , the anisotropy factor (or *g*-factor), defined as  $g = \Delta\epsilon/\epsilon$ , can be estimated from  $\theta/(33 \times A)$ , where  $\epsilon$  and *A* are the ordinary molar extinction coefficient and the absorbance under the conditions, respectively. Figure

(18) Negishi, Y.; Nobusada, K.; Tsukuda, T. *J. Am. Chem. Soc.* **2005**, *127*, 5261.  
(19) (a) Sosa, I. O.; Noguez, C.; Barrera, R. G. *J. Phys. Chem. B* **2003**, *107*, 6269. (b) Noguez, C. *Opt. Mater.* **2005**, *27*, 1204.

(20) Garzón, I. L.; Rovira, C.; Michaelian, K.; Beltrán, M. R.; Ordejón, P.; Junquera, J.; Sánchez-Portal, D. Artacho, E.; Soler, J. M. *Phys. Rev. Lett.* **2000**, *85*, 5250.  
(21) The containing running buffer solution interfered with the accurate CD measurements in the wavelength regions shorter than ~210 nm because of the high optical density of the solution. Hence, the spectra are shown from 210 to 700 nm. No CD signals were confirmed for the running buffer solution.  
(22) Kühnle, A.; Linderth, T. R.; Hammer, B.; Besenbacher, F. *Nature* **2002**, *415*, 891.

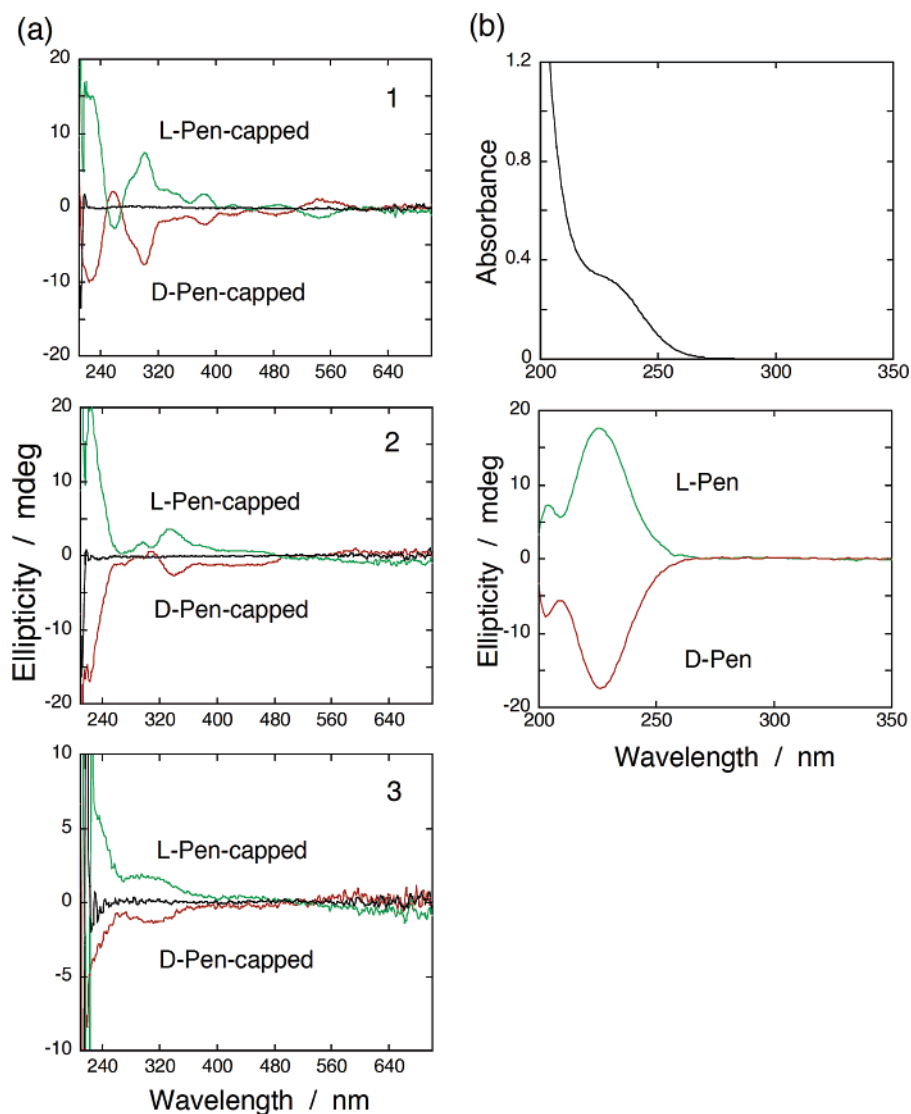


**Figure 4.** (a) CD spectra of each numbered gold nanocluster compound. Mirror image relationship in the CD signals between each numbered D-Pen-capped (red curve) and L-Pen-capped (green curve) gold nanoclusters can be seen. No CD signals were obtained for *rac*-Pen-capped gold nanoclusters (black curve). (b) Absorption (upper) and CD (lower) spectra of pure D-Pen and L-Pen in aqueous solution.

5 represents the anisotropy factor for compounds **1**–**3**. The *g*-factors of **1<sub>D</sub>** or **1<sub>L</sub>** are in the range of  $\pm 3 \times 10^{-4}$ , **2<sub>D</sub>** and **2<sub>L</sub>** in the range of  $\pm 2 \times 10^{-4}$ ; **3<sub>D</sub>** and **3<sub>L</sub>** in the range of  $\pm 1 \times 10^{-4}$ . The obtained *g*-factors for penicillamine-capped gold nanoclusters are approximately comparable to those for glutathione-capped gold nanoclusters obtained by Whetten and co-workers.<sup>7</sup> Furthermore, *g*-factors of our samples gradually decreased with increasing the cluster size (from 0.57 to 1.75 nm in diameter), different from the results by Whetten and co-workers; their *g*-factors were slightly increased from  $\pm 2 \times 10^{-4}$  to  $\pm 1 \times 10^{-3}$ , with an increase in the cluster sizes (from 0.7 to  $\sim 1.0$  nm), whereas larger species ( $> \sim 40$  Au atoms) show little optical activity.<sup>7</sup>

**Large Optical Activity of Penicillamine-Capped Gold Nanoclusters.** Typically, optically active chromophores are classified in two limiting cases:<sup>23</sup> (i) the inherently dissymmetric chromophore, and (ii) the inherently symmetric but dissymmetrically perturbed chromophore. The inherently dissymmetric

chromophore is one where the geometry of the chromophoric grouping lacks an  $S_n$  axis (improper axis of symmetry) represented by hexahelicene.<sup>2a</sup> On the other hand, the inherently symmetric chromophore is one where the symmetry of the isolated chromophore is sufficiently high to preclude optical activity. In this case, the chemical nature of the molecular environment and its alignment relative to the symmetry planes of the chromophore provide the associated rotational strength.

For gold nanoclusters covered with enantiopure penicillamine molecules, two major mechanisms can be considered for the appearance of such large optical activity based on the above considerations: (i) an inherently chiral core model, and (ii) a dissymmetric field model. The first one is that the origin of the chiroptical properties arises from inherently chiral or twisting atom-packing disordered structure in nanoclusters. Whetten and co-workers discussed this mechanism in detail for the large optical activity of glutathione-capped gold nanoclusters.<sup>8b</sup> Garzón and co-workers also discussed this model theoretically based on the calculation of the lowest-energy configurations of bare and methylthiolate-capped gold nanoclusters.<sup>6</sup> In the second

(23) Deutsche, C. W.; Lightner, D. A.; Woody, R.; Moscovitz, A. *Annu. Rev. Phys. Chem.* **1969**, *20*, 407.



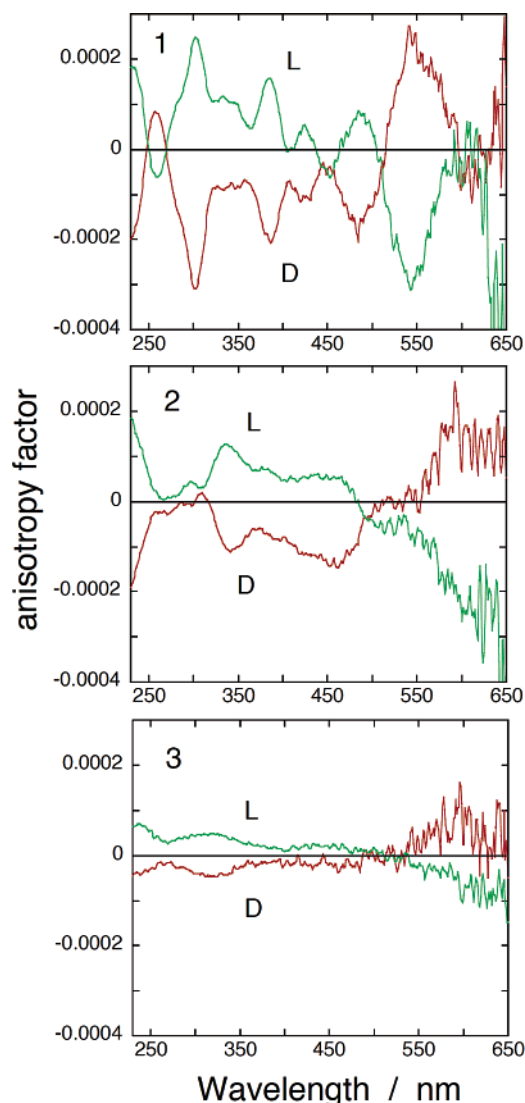


**Figure 5.** Anisotropy factor ( $g$ -factor) for each numbered gold nanocluster compound. The red and the green curves represent the D-Pen-capped and L-Pen-capped gold nanoclusters, respectively.

mechanism, on the other hand, the optical activity is induced by the electronic interactions between the achiral gold core and the chiral surface modifiers. The dissymmetric environment acts as a perturbing field electrostatically to break down the symmetry of the electronic state of nanoclusters as is observed for chiral  $d$ -metal complexes.<sup>2</sup>

We can first rule out the influence of the reduced number of atoms on the appearance of optical activity of gold nanoclusters. We prepared gold nanoclusters ( $\sim 0.6$  nm in diameter) covered with *meso*-2,3-dimercaptosuccinic acid (DMSA) in a similar method described here (see Supporting Information).<sup>24</sup> Note that *meso* compounds are optically *inactive* compounds that contain chiral carbons but can be superimposed on their mirror images. No CD signals were observed for the cluster samples. Therefore, the surface modifiers definitely affect the chiroptical properties of small gold nanoclusters.

Next, we will consider a model of the chiral gold core formation by a chiral surface modifier. During the cluster growth, if the D-form capping agent (such as D-Pen) induces a

specific helicity of gold atoms within the nanoclusters and the L-form (such as L-Pen) induces the opposite helicity, asymmetric induction, that is, conversion of optically inactive gold metals into chiroptical products, should be observed. This assumption or situation would lead to the appearance of large optical activity based on the inherently core model and can produce respective nanocluster enantiomers under the same kinetic processes.<sup>25</sup> Under the assumption, if the racemic mixture of the surface modifier is used for preparing gold nanoclusters, (i) each of enantiomers of the surface modifier will produce the respective homochiral gold nanoclusters with opposite core chirality, resulting in the formation of the mixture (or conglomerate) of gold nanocluster enantiomers, or (ii) statistical ligation of racemic thiols onto gold surfaces will produce gold nanoclusters having various stereostructures, resulting in the formation of the intrinsic racemic compounds. Under the condition of the statistical adsorption of racemic thiols (ii above), as is commonly observed,<sup>22</sup> different kinetic processes would be expected, yielding nanoclusters with different stereochemistry.<sup>26</sup> Such process will produce an ensemble of the *rac*-Pen-capped gold nanoclusters with different physical properties of size or chemical composition from those for the D-Pen-capped or L-Pen-capped gold nanoclusters.<sup>27</sup> A specific rearrangement of core gold atoms in the cluster may produce the lowest-energy configurations through an inhomogeneous electromagnetic field of the surface modifiers.<sup>6</sup> If the rearrangement is present, the core structure in the *rac*-Pen-capped gold nanoclusters should have higher and different symmetry within the chiral core model compared to that in the D-Pen-capped or L-Pen-capped gold nanoclusters because the *rac*-Pen-capped gold nanoclusters did not exhibit any optical activity. Hence, the core rearrangement in the *rac*-Pen-capped gold nanoclusters will also cause different physical or optical properties from those of the chiral-Pen-capped gold nanoclusters. On the contrary, the prepared *rac*-Pen-capped gold nanoclusters showed the same physical properties with D-Pen-capped or L-Pen-capped clusters: the same band positions in the PAGE separation and optical absorption (that implies the same size and chemical compositions). The above discussion indicates that contribution of inherently chiral core mechanism (or naturally helical structure) to the origins of large optical activity of penicillamine-capped gold nanoclusters is very small.

On the other hand, a dissymmetric field model can reasonably explain such a relatively large optical activity or anisotropy factor of penicillamine-capped gold nanoclusters. In transition metal complexes, such as  $[\text{Co}(\text{en})_3]^{3+}$ , the chiral arrangement of the chelate rings contributes to its optical activity in the region

- (25) (a) Kitamura, M.; Tokunaga, M.; Noyori, R. *J. Am. Chem. Soc.* **1993**, *115*, 144. (b) The processes are based on “kinetic enantioselectivity” which means that the rate of reaction caused by one enantiomer is different from that by the other enantiomer.
- (26) Recent theoretical calculations (ref 6) suggest that (i) chiral core structures have been obtained for bare  $\text{Au}_{28}$  and  $\text{Au}_{55}$  clusters; (ii) the chirality (Hausdorff chirality measure as a theoretical index of chirality) increases upon surface passivation; for example, methylthiolate-capped  $\text{Au}_{28}$  clusters with  $C_1$  symmetry show larger index of chirality than the corresponding bare  $\text{Au}_{28}$  clusters; (iii) the chirality decreases with increasing the cluster size. In the *absence* of statistical adsorption of racemic penicillamine molecules onto gold surfaces, that is, if each of enantiomers of penicillamine exclusively produces the respective homochiral gold nanoclusters with opposite core chirality, the predictions (i)–(iii) would support our results on penicillamine-capped gold nanoclusters. Although such situation seems unlikely (compare ref 22), we cannot fully rule out the influence of the core geometry.
- (27) Kagan, H. B.; Luukas, T. O.; Jacobsen, E. N.; Pfaltz, A.; Yamamoto, H. *Comprehensive Asymmetric Catalysis I*; Springer: Heidelberg, 1999.

(24) Negishi, Y.; Tsukuda, T. *J. Am. Chem. Soc.* **2003**, *125*, 4046.



of  $d-d$  absorption, called *conformational* effect. When the ligands contain chiral centers, optical activity is also induced from the transmission through space and by way of the chemical bonds linking the asymmetric center to the chromophore, called *vicinal* effect. The order of magnitude of the conformational effect depends on the chelate-ring puckering and that of the vicinal effect on the number of atoms between the asymmetric center and the central metal.<sup>28</sup> In the absence of chelation by the surface modifier of penicillamine, we might rule out the conformational effects on the observed optical activity. Then the most plausible explanation would lie in the vicinal effects. For transition metal complexes containing optically active ligands such as amino acids, relatively strong vicinal effects are observed. For example, the Co(III) complex of L-amino acid  $[\text{Co}(\text{NH}_3)_5(\text{L-valH})]^{3+}$  (L-valH: zwitterionic L-valine as a unidentate ligand) or  $[\text{Co}(\text{NH}_3)_4(\text{L-val})]^{2+}$  (L-val: basic L-valine as a bidentate ligand) exhibits a large  $g$ -factor of  $\sim 7 \times 10^{-4}$  or  $\sim 3 \times 10^{-3}$  in the visible light region, respectively.<sup>28b</sup> Such large optical activity has been explained in terms of the vicinal effect of chiroptical amino acids, and the hindered rotation of the ligands enhances its strength.<sup>28</sup> The penicillamine-capped gold nanoclusters, which have been demonstrated to behave like an optically active molecular complex, have magnitudes in the  $g$ -factor similar to those for the transition metal complexes described above, so that we believe that the chiroptical properties in compounds **1<sub>D</sub>**–**3<sub>D</sub>** and **1<sub>L</sub>**–**3<sub>L</sub>** essentially arise from the vicinal effect. The observed cluster size dependence of optical activity for the penicillamine-capped gold nanoclusters (that is, increase in optical activity with a decrease in cluster size) can be also explained by the effect because the efficiency of such vicinal effect depends on transmission through space within the linking asymmetric center to the chromophore.<sup>28</sup> When the nanocluster has a larger surface-to-volume ratio (that is, smaller cluster size), dissymmetric field induced by the surface chiral modifier would influence the electronic states of the core metal part more greatly, yielding larger  $g$ -factor or optical activity. On the basis of our results, we think that a pair of metal nanocluster

enantiomers can provide a novel future strategy for the chiral detection or molecular interaction analysis of biomolecules and create a new generation of photosensitive materials with controlled optical properties for optoelectronics and information recording.

#### 4. Conclusion

Gold nanocluster enantiomers protected by a pair of optically active penicillamine (D-Pen or L-Pen) were prepared. The mirror image relationship of CD signals was confirmed between the D-Pen-capped and the L-Pen-capped gold nanoclusters, suggesting that optically active surface modifier acts as a chiral selector, and that the nanoclusters have well-defined stereostructures as common molecules do. This finding will be important both for various spectroscopic diagnostics and for chiral detection or molecular interaction analysis in biochemistry. These chiroptical properties were investigated for the three separated fractions of gold nanoclusters by polyacrylamide gel electrophoresis (PAGE). Each fractionated component has the mean diameter of 0.57, 1.18, or 1.75 nm that was determined by SAXS analyses. With a decrease in the mean cluster diameter, optical activity or anisotropy factor gradually increased. The origins of the observed optical activity has been considered to be due to vicinal effects that come from dissymmetric field transmission through space and by way of the chemical bonds linking the dissymmetric center to the chromophoric gold core.

**Acknowledgment.** Prof. T. Okuyama and Dr. M. Fujita (University of Hyogo) are acknowledged for allowing us to use the CD spectropolarimeter. We also thank Dr. H. Koike (University of Hyogo) for providing significant information on the PAGE separations. The present work was financially supported by Grant-in-Aids for Scientific Research (S: 16101003, from MEXT), Scientific Research in Priority Areas: Application of Molecular Spins (15087210, from MEXT), and a grant from Kawanishi Memorial Shinmeiwa Education Foundation.

**Supporting Information Available:** FT-IR spectra and experimental details (optical and CD spectra, SAXS profile) about the DMSA-capped gold nanoclusters. This material is available free of charge via the Internet at <http://pubs.acs.org>.

JA053504B

(28) (a) Pessoa, J. C.; Gajda, T.; Gillard, R. D.; Kiss, T.; Luz, S. M.; Moura, J. J. G.; Tomaz, I. Telo, J. P.; Török, I. *J. Chem. Soc., Dalton Trans.* **1998**, 3587. (b) Yasui, T.; Hidaka, J.; Shimura, Y. *Bull. Chem. Soc. Jpn.* **1966**, 39, 2417.